POLITECNICO DI TORINO
Repository ISTITUZIONALE

Advanced cooling of the coaxial insert in high-power coaxial gyrotrons for fusion machines

Original
Advanced cooling of the coaxial insert in high-power coaxial gyrotrons for fusion machines / Zocaro, A., Katsara, E., Avramidis, K.A., Savoldi, L.. - In: FUSION ENGINEERING AND DESIGN. - ISSN 0920-3796. - ELETTRONICO. - 230:(2026). [10.1016/j.fusengdes.2026.115891]

Availability:
This version is available at: 11583/3015115 since: 2026-09-02T16:12:38Z

Publisher:
Elsevier Ltd

Published
DOI:10.1016/j.fusengdes.2026.115891

Terms of use:

This article is made available under terms and conditions as specified in the corresponding bibliographic description in the repository

Publisher copyright

(Article begins on next page)

26 November 2026

Fusion Engineering and Design 230 (2026) 115891

Contents lists available at ScienceDirect

Fusion Engineering and Design

journal homepage: www.elsevier.com/locate/fusengdes

Advanced cooling of the coaxial insert in high-power coaxial gyrotrons for fusion machines☆

Ariel Zocaro [a,*], Elena Katsara [b], Konstantinos A. Avramidis [b], Laura Savoldi [a,*]

[a] MAHTEP Group, Dipartimento Energia "Galileo Ferraris", Politecnico di Torino, Torino, 10129, Italy
[b] Department of Physics, National and Kapodistrian University of Athens, Zografou, Athens, 15784, Greece

ARTICLE INFO

Keywords:
Fusion
Gyrotron
Coaxial cavity insert
Cooling
TPMS

ABSTRACT

In high-power Electron Cyclotron Heating systems for fusion applications, coaxial-cavity gyrotrons enable improved mode control and higher output power compared to conventional hollow-cavity designs, but impose severe thermal loads on the coaxial insert. Advanced cooling solutions are therefore required to sustain higher ohmic heat fluxes without modifying the external geometry of the component. This work investigates innovative internal cooling layouts for the coaxial insert of a 2 MW, 170 GHz gyrotron cavity operating under single-phase coolant conditions. An integrated multiphysics framework is adopted, coupling electrodynamic simulations for the evaluation of ohmic losses with thermo-hydraulic and thermo-mechanical analyses to assess thermal performance, pressure drop, coolant phase stability, and structural integrity. Starting from a fin-based reference configuration, the cooling layout is progressively upgraded by introducing longitudinal fins and advanced architected geometries based on Triply Periodic Minimal Surfaces (TPMS), namely Gyroid and Split-P. The different configurations are systematically compared in terms of maximum sustainable heat flux and associated hydraulic and mechanical constraints. The results show that TPMS-based layouts significantly outperform conventional finned solutions. Compared to a fin-based configuration with enlarged return channel, the Gyroid and Split-P designs increase the maximum sustainable heat flux by more than 45% and 70%, respectively, while maintaining acceptable margins to boiling and thermo-mechanical deformation. Among the investigated options, the Gyroid-based layout provides the most favorable balance between heat transfer enhancement and pressure drop. Overall, the study demonstrates that advanced internal cooling layouts can substantially extend the heat flux handling capability of coaxial gyrotron inserts, supporting the development of next-generation high-power gyrotrons for fusion applications.

1. Introduction

Electron Cyclotron Heating (ECH) systems play a key role in plasma heating and current drive for present and future nuclear fusion devices. The increasing power demands of next-generation tokamaks and stellarators require gyrotrons capable of operating at multi-megawatt power levels in long-pulse or continuous-wave regimes. In this context, coaxial-cavity gyrotrons, see Fig. 1, have emerged as a promising alternative to conventional hollow-cavity designs. They offer in fact improved mode competition control and enable higher output power, maintaining acceptable thermal loads on the cavity wall [1].

A major challenge associated with the coaxial-cavity concept is the thermal management of the coaxial insert, which is subjected to intense and highly non-uniform ohmic heat fluxes. Excessive temperature increase or thermo-mechanical deformations of the insert can adversely affect both the cooling and electromagnetic performance, potentially leading to frequency shifts and loss of performance. Previous studies have demonstrated the feasibility of actively cooled coaxial inserts using conventional internal channel layouts [2,3]. However, these solutions exhibit limited scalability when higher thermal loads are required, as expected for future high-power gyrotrons. In particular, increasing the allowable heat flux without modifying the external geometry of the insert remains an open issue.

In high-temperature energy applications, it has been shown that the introduction of internal flow-driving structures can significantly enhance heat transfer performance by increasing the wetted surface area and promoting flow mixing [5]. More recently, Triply Periodic Minimal Surface (TPMS) geometries have attracted considerable attention due to their high surface-to-volume ratio, interconnected porosity, and favorable thermo-mechanical behavior, enabling substantial heat transfer

☆ This article is part of a Special issue entitled: 'ISFNT-16' published in Fusion Engineering and Design.

* Corresponding authors.
E-mail addresses: ariel.zocaro@polito.it (A. Zocaro), laura.savoldi@polito.it (L. Savoldi).

https://doi.org/10.1016/j.fusengdes.2026.115891
Received 30 December 2025; Received in revised form 1 June 2026; Accepted 16 June 2026
Available online 22 June 2026
0920-3796/© 2026 The Authors. Published by Elsevier B.V. This is an open access article under the CC BY license (http://creativecommons.org/licenses/by/4.0/).

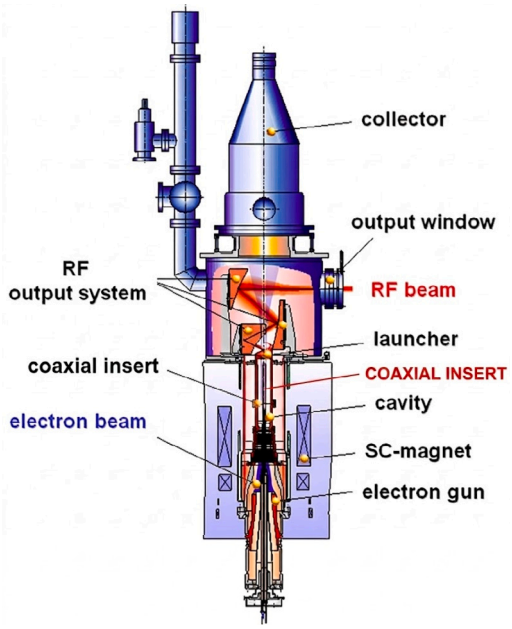

Fig. 1. Sketch of the 2 MW 170 GHz KIT coaxial-cavity gyrotron (modified from [4]), where the insert is shown.

enhancements compared to conventional finned configurations [6–9]. Despite these promising results, the potential of TPMS-based cooling layouts has not been systematically explored for gyrotron components yet, in particular for coaxial cavity inserts operating under extreme thermal loads.

The objective of this work is to assess innovative internal cooling layouts for the coaxial insert of a 2 MW, 170 GHz gyrotron cavity without modifying its external geometry. An integrated multiphysics framework is employed, combining electrodynamic simulations to determine the spatial distribution of ohmic losses with thermo-hydraulic and thermo-mechanical analyses to evaluate thermal performance, coolant phase stability, pressure losses, and structural integrity. Several cooling configurations are investigated and compared, including conventional longitudinal fins and advanced TPMS-based geometries. The results aim to demonstrate the potential of advanced internal layouts to significantly increase the allowable heat flux, thereby supporting the development of next-generation high-power coaxial-cavity gyrotrons for fusion applications.

2. Cooling configurations

The initial geometry of the gyrotron coaxial insert is provided by the Karlsruhe Institute of Technology (KIT) as a complete CAD model. The insert is a Glidcop component with a total length of 1339 mm, extending from the base of the gyrotron and fully crossing the cavity region. Its outer surface includes a corrugated section composed of 76 grooves with a depth of 0.44 mm, designed to satisfy the electromagnetic requirements of the coaxial cavity.

The original internal cooling layout, previously investigated in [2, 3], consists of a central circular inlet channel with a radius of 3 mm, through which the coolant enters the cavity region. In the upper part of the insert, four rectangular channels guide the flow into an outer annular return passage with a thickness of 1 mm. This configuration represents the reference geometry from which all subsequent modifications and upgrades are developed.

In high-temperature energy applications, it has been shown that the introduction of internal flow-guiding structures can significantly enhance heat transfer performance in tubular systems by increasing the effective heat exchange area and promoting flow mixing. In particular, Ebadi et al. [5] demonstrated that a concentric double-pass configuration implemented in a geometry closely resembling that of the coaxial cavity insert can significantly improve the device thermal performance through the use of simple longitudinal fins connecting the inner and outer shells. Inspired by this concept, the original recirculation channels of the coaxial insert are removed and replaced with longitudinal fins, defining the first upgraded configuration (Case 1), shown in Fig. 2(a). Several fin arrangements were evaluated by varying both the number of fins and their thickness. Among the tested options, the configuration featuring six fins with a thickness of 2 mm was identified as the most promising, offering the best overall compromise between heat transfer enhancement, pressure drop, and manufacturability. This configuration is therefore selected as the baseline for the subsequent analyses.

A second configuration (Case 2), shown in Fig. 2(b), builds upon the fin-based layout of Case 1 by increasing the thickness of the coolant return channel in order to mitigate potential issues related to flow interference or blockage. Specifically, the thickness of the annular return channel is increased by 3 mm by reducing the radius of the inner inlet conduit by 1 mm and decreasing the thickness of the outer wall of the coaxial insert by 1 mm. The number and thickness of the longitudinal fins are kept identical to those of Case 1, enabling a direct assessment of the impact of the return channel geometry on the thermal and hydraulic performance.

Two additional configurations are investigated by replacing the longitudinal fins with architected structures based on Triply Periodic Minimal Surfaces (TPMS), featuring an annular cylindrical profile. In particular, a Gyroid-based geometry is adopted in Case 3 (Fig. 2(c)), while a Split-P TPMS configuration is considered in Case 4 (Fig. 2(d)) [10]. The unitary cells of the two topologies are shown in Fig. 3.

TPMS geometries are defined by periodic mathematical surfaces repeated in three spatial directions [11] and are characterized by high surface-to-volume ratios, interconnected porosity, and relatively uniform mechanical properties. These features make TPMS structures particularly attractive for advanced cooling and heat exchange applications [6,7].

Compared to conventional finned designs, TPMS-based heat sinks have demonstrated significantly enhanced heat removal capabilities, with reported performance improvements of up to 48%–61% under comparable operating conditions [8]. In the present study, both the fin-based configurations (Case 1 and Case 2) and the TPMS-based configurations (Case 3 and Case 4) are designed with a target global porosity of 60% to ensure a fair comparison between the different cooling concepts. To limit the pressure drop between the inlet and outlet of the cooling system, the TPMS geometries are locally modified by elongating the unit cells in regions subjected to lower thermal loads. Furthermore, a graded porosity distribution is introduced along the axial direction, with a porosity of 50% in the region of maximum heat flux and 75% toward the extremities of the insert. This design strategy aims to maximize heat transfer where it is most needed while avoiding excessive hydraulic losses in less critical regions.

The selected set of cooling configurations allows for a systematic comparison between conventional and advanced internal layouts, showing their direct impact on the maximum sustainable heat flux, pressure drop, and thermo-mechanical response of the coaxial insert.

3. Methodology for the analysis and simulation setup

The thermal performance of the coaxial insert is governed by a strong coupling between electromagnetic, thermal-hydraulic, and thermo-mechanical phenomena. In order to accurately capture these interactions, an integrated multiphysics workflow is adopted. The analyses are carried out using the MUCCA framework, which iteratively couples electrodynamic (ED), thermo-hydraulic (TH), and thermo-mechanical (TM) solvers [12].

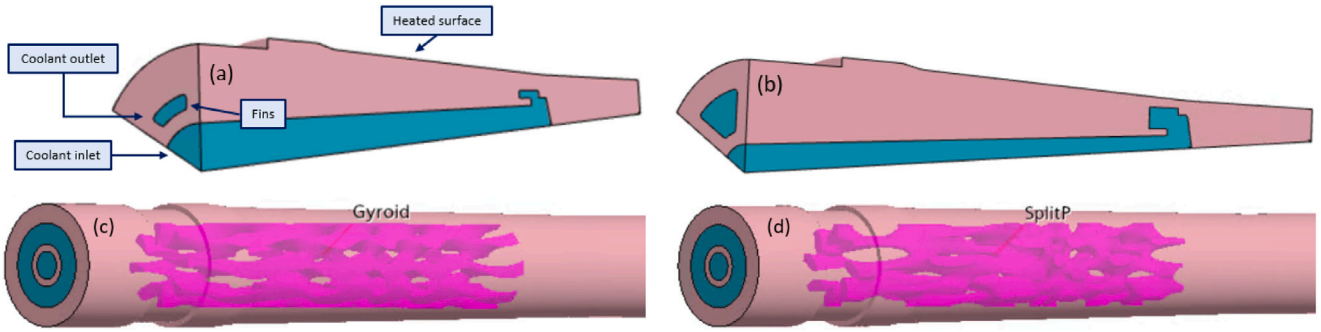

Fig. 2. Cooling configurations: longitudinal fins with a return channel thickness of 1 mm (a), longitudinal fins with a return channel thickness of 3 mm (b), TPMS Gyroid (c), and TPMS SplitP (d).

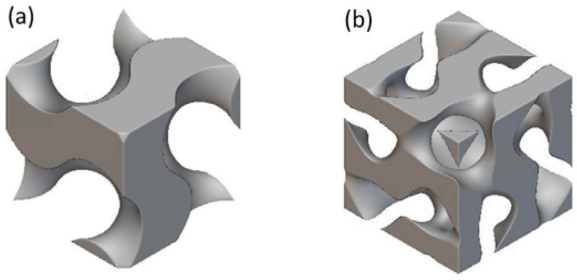

Fig. 3. TPMS unit cell: Solid Gyroid (a) and Solid SplitP (b).

The workflow is initiated by the electrodynamic solver EURIDICE [13], which computes the spatial distribution of the ohmic heat load on the coaxial insert surface. This heat flux distribution represents the starting point for the thermo-hydraulic analysis. The resulting temperature field and pressure distribution are subsequently transferred to the thermo-mechanical solver to evaluate the induced stresses and deformations. The deformed geometry is then fed back to the electrodynamic solver, and the loop is repeated until convergence of the heat flux distribution is achieved. This iterative procedure ensures a consistent representation of the coupled physical phenomena affecting the gyrotron cavity insert. The coupled multiphysics workflow is applied iteratively to each configuration in order to determine the limit heat flux distribution along the coaxial insert. The limiting condition is defined as the highest heat load that can be sustained without inducing phase change of the coolant anywhere within the cooling domain, under the prescribed mass flow rate and inlet pressure conditions.

3.1. Thermo-hydraulic simulation setup

The thermal-hydraulic simulations are performed using STAR-CCM+ to solve the steady-state, three-dimensional conjugate heat transfer problem. The solid domain is modeled as Glidcop, with temperature-dependent thermal conductivity and specific heat defined through polynomial correlations [14]. A segregated solid-energy model is employed to compute the thermal response of the insert.

The coolant, liquid water in turbulent regime, is simulated using a steady-state Reynolds-Averaged Navier–Stokes (RANS) approach with the k–ω SST turbulence model. Momentum and energy conservation equations are solved using a segregated flow solver, while temperature-dependent fluid properties are accounted for through the IAPWS-IF97 formulation [15]. Near-wall effects are resolved using an all-y^+ wall treatment, ensuring accurate prediction of both velocity and thermal boundary layers.

At the inlet, a constant mass flow rate of $\dot{m} = 0.165$ kg/s is imposed, consistent with values adopted in previous studies on similar geometries [2,3]. Note that this value is experimentally determined as the value allowing operation without significant vibration [3]. For the fin-based configurations (Case 1 and Case 2), geometric symmetry allows only one-sixth of the domain to be simulated, with the mass flow rate scaled accordingly. Conversely, for the TPMS-based configurations (Case 3 and Case 4), the full cooling domain is modeled, and the total mass flow rate is applied. The inlet velocity is computed as

$$v = \frac{\dot{m}}{\rho A}, \tag{1}$$

where ρ is the fluid density and A is the inlet cross-sectional area. As a result, configurations featuring an inlet radius of 2 mm (Case 2, Case 3, and Case 4) operate at an inlet velocity of approximately 13.2 m/s, while Case 1, retaining the original inlet radius, exhibits a lower inlet velocity of about 5.9 m/s.

The outlet pressure is adjusted such that the absolute pressure at the inlet of the coaxial insert within the cavity region reaches $p_{\text{inlet}} = 5.1$ bar, consistent with realistic operating conditions of the cooling system. An initial uniform temperature of 40 °C is imposed on both solid and fluid domains to ensure thermal equilibrium prior to the application of the heat load.

The heat flux distribution obtained from the electrodynamic simulations is applied as a boundary condition on the outer surface of the coaxial insert (Fig. 4). A cylindrical coordinate system is employed to accurately map the spatially varying heat flux onto the curved surface of the insert.

The computational mesh is generated using an automated polyhedral mesher, complemented by surface remeshing and the insertion of prism layers to adequately resolve near-wall gradients. Local mesh refinement is applied within the fluid channels to improve the accuracy of the predicted velocity and temperature fields. Solution verification guarantees a small numerical uncertainty on the computed results.

3.2. Thermo-mechanical simulation setup

Following the thermo-hydraulic analysis, a thermo-mechanical simulation is performed to assess stresses and deformations of the coaxial insert and to verify their compatibility with gyrotron operational requirements. The temperature field obtained from the thermo-hydraulic simulation is mapped onto the solid domain and used as the thermal load for the structural analysis.

The solid region is discretized using a tetrahedral mesh with a characteristic cell size of 0.5 mm, with additional refinement applied in the thin solid wall separating the inner and outer fluid regions. Mechanical boundary conditions are imposed by constraining the base of the insert, while the remaining surfaces are left free to deform.

The thermo-mechanical analysis employs a steady-state three-dimensional solid stress model based on the finite element method. The material behavior of Glidcop is described using isotropic linear elasticity and isotropic thermal expansion, with temperature-dependent

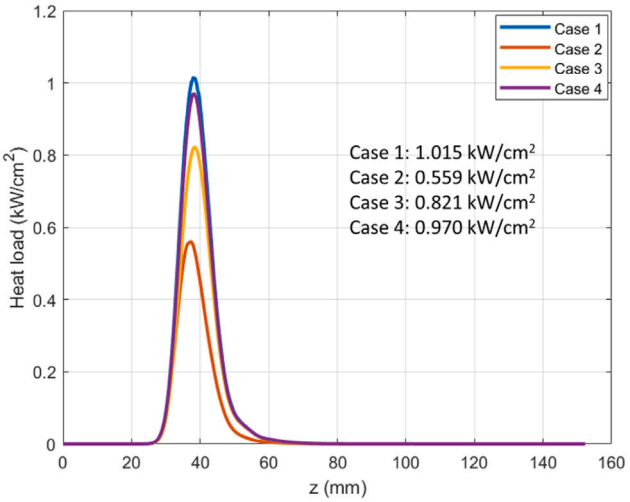

Fig. 4. Limit ohmic load axial distribution along the coaxial insert for the four considered case.

Table 1
Maximum temperatures reached in the fluid and solid regions and pressure drop for the analyzed cases.

Case	Peak heat flux (kW/cm^2)	Total absorbed thermal power (kW)	Max fluid temperature (°C)	Max solid temperature (°C)	Pressure drop (bar)
1	1.015	5.584	152.6	221.5	0.7
2	0.559	3.053	140.9	162.6	1.2
3	0.821	4.644	143.3	176.8	1.6
4	0.970	5.406	136.5	174.5	2.7

properties, including density, Young's modulus, and thermal expansion coefficient, defined according again to [14]. The resulting displacement and stress fields are used to assess the structural integrity of the insert and to ensure that deformations remain within acceptable limits for proper gyrotron operation.

4. Results

This section compares the thermo-hydraulic performance of the four cooling configurations in terms of maximum sustainable ohmic heat load, pressure drop, and margin to boiling. These quantities represent the key performance metrics for comparing conventional fin-based solutions with advanced TPMS-based cooling layouts.

As shown in Fig. 5, the temperature distribution within the fluid region closely follows the spatial trend of the applied heat load for all the analyzed configurations. It can also be observed that, in the regions subjected to higher thermal loads, smaller TPMS cell heights were adopted, whereas in areas characterized by lower temperatures the structure was stretched in order to limit the pressure drop that would otherwise result from more tortuous geometries.

Table 1 reports the maximum temperatures computed in the fluid and solid regions. In all cases, the highest temperatures in the solid domain are reached on the heated surface in correspondence to the peak heat load.

Case 1 exhibits the lowest pressure drop, while Case 4 shows the highest pressure losses due to the increased flow tortuosity of the TPMS structure. Nevertheless, it can be observed that, in the case of the Gyroid TPMS configuration, the pressure drop can still be maintained at a level comparable to that of Case 2, which features fins with the same diameter geometry. Case 2, featuring fins, shows a higher pressure drop than Case 1 due to the reduction of the fluid inlet cross section; at the same mass flow rate, this results in a higher inlet water velocity and, consequently, an increased pressure drop.

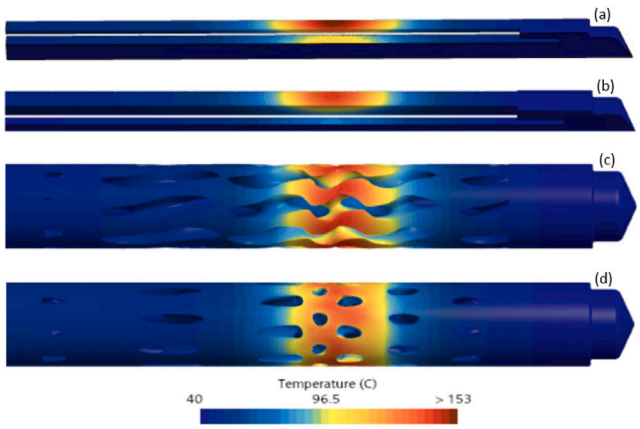

Fig. 5. Fluid temperature distribution: case 1 (a), case 2 (b), case 3 (c), and case 4 (d).

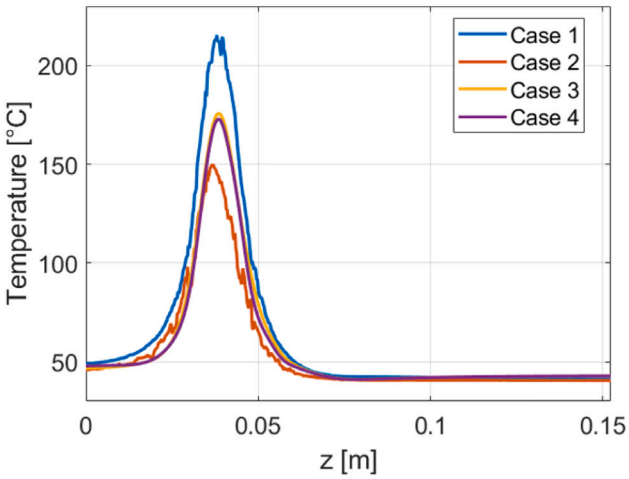

Fig. 6. Longitudinal temperature distribution of the heated surface.

Fig. 6 shows the longitudinal temperature distribution of the heated surface. The maximum temperature is attained in Case 1. It can also be observed that the maximum solid temperature reached in Case 4 is significantly lower than that of Case 1, despite the absorbed thermal powers being very similar. This result highlights the excellent thermal performance of TPMS structures compared with simpler solutions such as longitudinal fins.

Given the maximum fluid temperatures approaching 140 °C, the potential onset of boiling is assessed. Therefore, the analysis focuses on evaluating the local saturation conditions of the coolant by considering the combined effect of fluid temperature and absolute total pressure in the regions of interest. In the areas where the fluid reaches its highest temperature, which are located at the interface with the heated surface, the absolute total pressure remains well above atmospheric conditions, exceeding 1 bar (Fig. 7) and is taken as the reference level for assessing the risk of phase change.

Investigating possible boiling phenomena is limited to regions where the fluid temperature exceeds 100 °C, as under the pressure conditions considered this may indicate the onset of nucleate boiling.

The surface tension, vapor density, and latent heat were calculated using a MATLAB script, which takes the total pressure as input. Subsequently, the saturation temperature of water at that pressure value was evaluated.

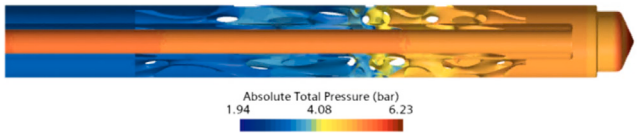

Fig. 7. Absolute total pressure distribution for case 4.

Table 2
Thermophysical properties of the coolant and the margin to boiling.

Case	Latent heat (kJ/kg)	Surface tension (N/m)	Vapor density (kg/m^3)	$T_{sat} - T_{max}$ (K)
1	2068	0.0457	3.593	6.8
2	2105	0.0481	2.727	10.2
3	2109	0.0484	2.637	6.5
4	2117	0.0491	2.475	9.2

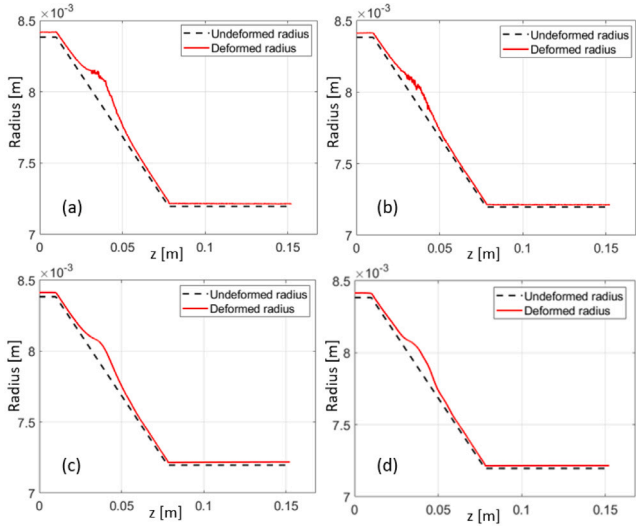

Fig. 8. Radial displacement: case 1 (a), case 2 (b), case 3 (c), and case 4 (d).

Table 3
Maximum displacements and maximum Von Mises stress on the heated surface for the analyzed cases.

Case	Max radial displacement (m)	Max axial displacement (m)	Max stress heated surface (MPa)
1	2.02×10^{-5}	9.08×10^{-5}	125.5
2	1.47×10^{-5}	7.22×10^{-5}	105.4
3	1.49×10^{-5}	8.11×10^{-5}	113.7
4	1.35×10^{-5}	7.82×10^{-5}	162.3

Table 2 shows the values of latent heat, surface tension, and vapor density of the coolant to evaluate the margin to phase change at the interface with the heated surface. As can be observed, in all four cases the difference between the saturation temperature and the maximum fluid temperature is positive, indicating that no phase change of the coolant occurs. In all cases, a safe margin of a few degrees is maintained.

Fig. 8 shows the radial displacement on the heated surface, magnified by a factor of 10. It can be observed that, near the maximum thermal load, the deformation exhibits nonlinear behavior. In all cases, the maximum radial displacement occurs in proximity to the region of maximum heat load. The maximum radial and axial displacement values, reported in Table 3, remain within safe operational limits, as do the maximum stress values on the heated wall of the insert.

5. Conclusions

This work investigated advanced internal cooling layouts for the coaxial insert of a 2 MW, 170 GHz gyrotron cavity, with the aim of increasing the maximum sustainable ohmic heat flux without modifying the external geometry of the component. An integrated multiphysics framework, coupling electrodynamic, thermo-hydraulic, and thermo-mechanical analyses, was employed to consistently assess thermal performance, coolant phase stability, pressure losses, and structural integrity. The results demonstrate that the introduction of internal flow-driving structures can substantially enhance the thermal performance of the coaxial insert. Among the conventional solutions, longitudinal fins significantly increase the allowable heat load compared to the reference configuration, while maintaining single-phase coolant conditions and acceptable thermo-mechanical deformations. Increasing the thickness of the return channel represents a viable design option to mitigate potential flow interference, albeit at the expense of a moderate reduction in thermal performance. When advanced cooling configurations are considered, TPMS-based cooling layouts clearly outperform conventional finned designs under comparable geometric constraints. In particular, the Gyroid and Split-P configurations increase the maximum sustainable heat flux by more than 45% and 70%, respectively, relative to the fin-based configuration with enlarged return channel, while preserving adequate margins to boiling and structural deformation. These performance gains are primarily attributed to the high surface-to-volume ratio and enhanced flow mixing inherent to TPMS structures. The analysis also highlights the trade-off between thermal performance and hydraulic losses. While the Split-P configuration achieves the highest heat flux capability, it is associated with a significant pressure drop. Conversely, the Gyroid-based layout provides the most favorable balance between heat transfer enhancement and hydraulic losses, making it a particularly attractive solution for practical implementation in high-power gyrotron cooling systems.

CRediT authorship contribution statement

Ariel Zocaro: Writing – original draft, Visualization, Validation, Software, Methodology, Investigation, Formal analysis, Data curation, Conceptualization. **Elena Katsara:** Writing – review & editing, Software, Methodology. **Konstantinos A. Avramidis:** Writing – review & editing, Supervision, Software, Methodology, Funding acquisition, Conceptualization. **Laura Savoldi:** Writing – review & editing, Supervision, Resources, Project administration, Methodology, Funding acquisition, Conceptualization.

Declaration of competing interest

The authors declare that they have no known competing financial interests or personal relationships that could have appeared to influence the work reported in this paper.

Acknowledgments

This work was funded by the EUROfusion Consortium.

Data availability

Data will be made available on request.

References

[1] Z.C. Ioannidis, K.A. Avramidis, I.G. Tigelis, Selectivity properties of coaxial gyrotron cavities with mode converting corrugations, IEEE Trans. Electron Devices 63 (2016) 1299–1306.

[2] A. Bertinetti, F. Albajar, K.A. Avramidis, F. Cau, F. Cismondi, G. Gantenbein, J. Jelonnek, P.C. Kalaria, S. Ruess, T. Rzesnicki, L. Savoldi, R. Zanino, Analysis of an actively-cooled coaxial cavity in a 170 ghz 2 mw gyrotron using the multi-physics computational tool mucca, Fusion Eng. Des. 146 (2019) 74–77.

[3] P.C. Kalaria, M. George, S. Illy, K.A. Avramidis, G. Gantenbein, S. Ruess, M. Thumm, J. Jelonnek, Multiphysics modeling of insert cooling system for a 170-ghz, 2-mw long-pulse coaxial-cavity gyrotron, IEEE Trans. Electron Devices 66 (2019) 4008–4015.

[4] S. Ruess, G. Gantenbein, S. Illy, J. Jelonnek, A. Samartsev, M. Thumm, Kit coaxial gyrotron development: from iter toward demo, J. Plasma Phys. (2018) Published online: 05 2018.

[5] H. Ebadi, A. Cammi, L. Savoldi, Energetic and exergetic analyses of a double-pass tubular absorber for application in solar towers, ASME J. Sol. Energy Eng. 146 (2024) 051013.

[6] K. Dutkowski, M. Kruzel, K. Rokosz, Review of the state-of-the-art uses of minimal surfaces in heat transfer, Energies 15 (2022) 7994.

[7] L. Zhang, et al., Energy absorption characteristics of metallic triply periodic minimal surface sheet structures under compressive loading, Addit. Manuf. 23 (2018) 505–515.

[8] N. Baobaid, M.I. Ali, K.A. Khan, R.K.A. Al-Rub, Fluid flow and heat transfer of porous tpms architected heat sinks in free convection environment, Case Stud. Therm. Eng. 33 (2022) 101944.

[9] L. Savoldi, et al., Use of triply periodic minimal surface lattices for heat transfer applications: A systematic literature investigation, Energies (2026).

[10] A. Mortazavi, A.L. Ávila-Marín, H. Ebadi, E. Gaietti, C. Piatti, L. Marocco, L. Savoldi, Experimental investigation of triply periodic minimal surfaces for high-temperature solar receivers, Case Stud. Therm. Eng. 60 (2024) 104771.

[11] H. Karcher, K. Polthier, Construction of triply periodic minimal surfaces, in: H.-C. Hege, K. Polthier (Eds.), Visualization and Mathematics, Springer, 1997, pp. 119–132.

[12] L. Savoldi, A. Bertinetti, Development of the Multi-Physics Tool for the Integrated Simulation of the Cavity and Its Application for the Design of Gyrotron Cavities for Thermonuclear Applications, (Ph.D. thesis), Politecnico di Torino, 2019.

[13] K.A. Avramides, I.G. Pagonakis, C.T. Iatrou, J.L. Vomvoridis, Euridice: A code-package for gyrotron interaction simulations and cavity design, in: EPJ Web of Conferences, vol. 32, 2012, 04016.

[14] J.W. Davis, G.W. Wille, S. Fabritsiev, ITER material properties handbook: DS Copper – Ultimate tensile strength https://www.iter.org/doc/www/materials File Code: ITER-AK04-2101, Publication Package (4) cited on 43 47, 58.

[15] Star-ccm+ user guide, version 2306 ed., siemens digital industries software, 2023, URL: https://support.sw.siemens.com/.